JOURNAL OF OPTOELECTRONICS AND ADVANCED MATERIALS Vol. 9, No. 2, February 2007, p. 438 - 441

The electroconvection in dimeric nematic liquid crystals

M. PETROV*, B. KATRANCHEV, E. KESKINOVA, H. NARADIKIAN
Institute of Solid State Physics, Bulgarian Academy of Sciences, 72 Tzarigradsko Chaussee Blvd., 1784 Sofia, Bulgaria.

The electroconvection (EC) in nematics with short range smectic C order, scanning both the high-temperature nematic region (N_1) and the low-temperature one (N_2), differentiated by a definite temperature T^*, was investigated. The influence of the change of the magnitude and the sign of the electroconductivity, σ_a, anisotropy, as well as the influence of the director ***n*** positions (both driven by temperature variation), on the EC mechanism and the corresponding optical patterns are discussed. The isotropic character of the EC instability initiated by the 'loss' of electroconductivity anisotropy below T^*, and in the vicinity of the nematic-isotropic phase transition, is discussed.

(Received Novemebr 28, 2006; accepted December 21, 2006)

Keywords: Liquid Crystals, Dimeric nematics, Electroconvection

1. Introduction

Electroconvection (EC) driven by an ac voltage is commonly observed in nematic (N) liquid crystals (LC) with a positive conductivity anisotropy ($\sigma_a=\sigma_{\|}-\sigma_{\perp}$) and a negative or slightly positive dielectric anisotropy ($\varepsilon_a=\varepsilon_{\|}-\varepsilon_{\perp}$), where $\|$ and $\perp$ mean parallel and perpendicular to the director ***n*** (the mean orientation of the molecules) respectively. The case $\sigma_a > 0$ and $\varepsilon_a < 0$ in the conventional Ns presents the EC in its classical variant, where the experiments and theory match very well [1-3].

In the conductive regime, one can observe normal rolls (NRs) with the wave vector ***q*** of the convection rolls parallel to the preferred 'easy' direction $\boldsymbol{n}_o$, defined as the *x* axis, and oblique rolls (ORs) which show a certain angle between ***q*** and $\boldsymbol{n}_o$. Increasing the electric field and changing its frequency, one also observes various secondary instabilities such as the zig-zag instability, the abnormal roll instability, and so on [4-6].

In [7,8], a kind of instability called the prewavy instability was reported. Although the prewavy and similar instabilities have been observed and discussed in experiment and theory [9,10], open questions and discrepancies still remain. Sometimes, the prewavy isotropic mode cannot be distinguished from the anisotropic dielectric mode observed above a cutoff frequency f_c.

The Ns, which appear before S_C phase at cooling display S_C order fluctuations. These fluctuations impose specific features on the EC. In these Ns, the competition between the homogeneous Freedericksz transition mode and the non-equilibrium EC mode was detected long ago [11]. Recently [12], we have discovered EC dendrite instability in such Ns similar, in microtextural aspects, to that described by Gleeson [13-15] in the convectional Ns in the presence of a strong magnetic field.

In the present paper, we focus on EC in Ns with short range S_C order, scanning both the high-temperature N region (N_1) and the low-temperature one (N_2) differentiated by a definite temperature T^*. The influence of the change in the magnitude and the sign of σ_a, as well as the influence of the director ***n*** positions (both driven by the temperature variation), on the EC mechanism and the corresponding optical patterns are discussed. The EC instability initiated by the 'loss' of electroconductivity and surface symmetry anisotropy, as well as the balance between the Carr-Helfrich (CH) and the 'isotropic' mechanisms, is discussed.

2. Experimental results

2.1. Sample preparation and microstructure analysis

We used the 7th homologue of 4,n-alkyloxybenzoic acids (7OBA), filled (in its isotropic phase) between two parallel glass plates whose surfaces were coated with transparent electrodes of indium tin oxide (ITO). The phase diagram of 7OBA is:

$$\mathrm{Cr} \xleftarrow{92^{o}\mathrm{C}} \mathrm{S_C} \xleftarrow{98^{o}\mathrm{C}} \mathrm{N} \xleftarrow{146^{O}\mathrm{C}} \mathrm{I}$$

The LC cell thickness d was 12 μm, measured by an interference method.

We used here the OXYZ laboratory coordinate system (OXY – the glass plate plane; Z – the normal to the plate). As a result of our microtextural and diffraction polarization analyses of the EC, we differentiated the N phase into three typical regions, revealing three detached EC patterns. These were $T_{NI}-5°C<T\leq T_{NI}$ (region I-R_I); $T^*<T<T_{NI}-5°C$ (region II-R_{II}) and $T<T^*<T_{NC}$ (region III-R_{III}). The EC in each of the regions is specific. This specificity is due to the significant change of the sign and the magnitude of σ_a and the angle Θ (between ***n*** and the substrate normal $\boldsymbol{k} \equiv z$) value upon temperature variation. The first noticeable feature, scanning the temperature, is that the ECs in R_I and R_{III} more or less obey the isotropic mechanism, while in the region R_{II} the EC is driven by the

CH mechanism. The 'loss' of the electrical and optical anisotropy of the LC system is due to the diminution of σ_a and the surface symmetry increase (from a planar ($\Theta = \pi/2$) through a conical ($\pi/2 > \Theta > 0$) to a homeotropic ($\Theta = 0$) orientation). Therefore the 'loss' of anisotropy favours the 'isotropic' [16] mechanism, while in contrast the 'gain' of anisotropy favours the CH (anisotropic) [1, 2] mechanism. The 'isotropic' one is very cursorily studied, although it is the focus of the most of the recent EC investigations [3-10].

In the temperature range $T < T^*$, when the quasi-layers form, σ_a drastically changes, since $\sigma_\perp$ (in the layer plane) is bigger than $\sigma_\parallel$ along $\boldsymbol{n}$ [1]. As a result, σ_a is < 0.

2.2. Microtextural polarization analysis

At a fixed temperature (T_{NI}–12°C) in the R_{II} region, we increased the voltage in order to start the EC instability. Instead of the expected NRs instability, typical for the conventional Ns, we obtained (after the Freedericksz transition) ORs instability, normally appearing as a second instability at very high electric fields. Further voltage increase led to very fast evolvution of ORs in zig-zag (ZZ) rolls. Thus, one finds a sequence of bifurcations: a Freedericksz transition → ORs → ZZ with increasing voltage.

Close to the T^* (T_{NI}-20°C), but still above T^*, just at the threshold $U_{th} \approx 40$V for 1kHz, we clearly observed spontaneously evolution into a sinusoidal wavy pattern. This pattern evolved into a propagating spiral one and finally into closed stripe lines, which we called 'cell-like domains', well seen in Fig. 1.

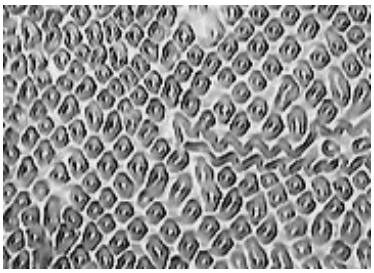

Fig. 1. The established cell-like domains.

By the far-field diffraction polarization analysis, one can follow both the EC structure and texture. The electrical driving of the instability is included in the wave vector $\boldsymbol{q}=2\pi/\lambda_{th}$ variation, λ_{th} - the wavelength at the threshold. λ_{th} is roughly of the order of d ($d < \lambda_{th} \leq 3d$). 1D far-field diffraction for two intersected ORs is shown in Fig. 2a. A 2D EC grating is presented in Fig 2b.

In the R_I region, the sequences of the EC rolls appearance and development is as follows: at the threshold for a corresponding frequency, we observed as the primary instability wide strip-like domains (Fig. 3) with $\boldsymbol{q}$ almost parallel to x ($\boldsymbol{q}\|\boldsymbol{n}$). Further voltage increase above the threshold led to a very small decrease in the wavelength, the oblique ($\boldsymbol{q}\neq\boldsymbol{n}$) director distortion and a tendency to closure of the stripe lines. In contrast to the lower temperature R_{II} region, the stripe lines in the R_I region do not reach closure i.e. 'cell-like domains' formation. We found by both optical methods that the $\lambda_{th}(f)$ and $\lambda_{th}(U)$ are $\approx 10d$. This is one of the symptoms that the CH mechanism (where the cell thickness d controls the EC wavelength) is broken in the high-temperature region R_I. We accepted the isotropic mechanism as a possible EC mechanism in this region. The authors in [7,8] also interpreted their observed prewavy EC instability, very similar in textural aspect to that in R_I region, by the isotropic mechanism (for details of this mechanism, see [9]). In Fig. 4, the diffraction pattern is an orthoscopic image of the $\boldsymbol{n}$ field. The Maltese cross is well seen. It confirms the homeotropic ($\Theta \approx 0$) LC orientation and indicates the increase in the surface isotropy i.e. the reduction in the surface as well as the σ_a anisotropies in the R_I region. We recall that we referred to the reduction in both the surface and σ_a anisotropies as the 'loss' of electrical and optical anisotropy of the LC system.

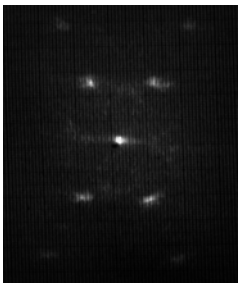

a

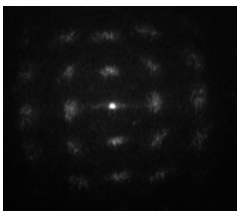

b

Fig. 2. a) Two intersected 1D diffraction patterns expressing two intersected ORs. b) 2D diffraction pattern obtained by the cell-like domains (Fig. 1). $T=T_{NI}$-18 °C, f=1kHz, U_{th}=22V.

Fig. 3. The wide stripe-like domains in the R_I region. $T = T_{NI}$-2 °C, f = 1 kHz, U_{th} = 36 V, d = 12μm, crossed polarizers, magnification 100x.

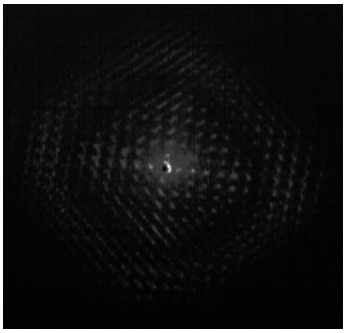

Fig. 4. The orthoscopic picture of the R_I region at $T=T_{NI}$-2 ℃, f=1kHz, U=30V, d=12μm.

In the R_{III} region, EC occurs above a strong Freedericksz transition. We observed an EC pattern (see. Fig. 5), which looks like the closed 'cell-like' stripe domains in Fig. 1. The difference, however, is in two aspects: (i). the EC, which is not predicted by the current EC theory, is a localized spatial temporal state; (ii). The EC pattern seems like a set of centered elongated dendrite-like domains.

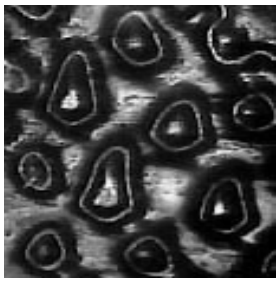

Fig. 5. The dendritic EC texture below T^* at f=1kHz, U=60V, $T=T_{NI}$-30 ℃, d=12μm, magnification 100x.

The wavelengths of the observed dendrite-like domains (including one white and one black stripe) are constant with U and frequency variations, similarly to those of the R_I region (4-6d). The EC in this region is also reminiscent of the isotropic one, resulting from the CH mechanism breaking.

The EC instabilities in R_I and partially in R_{II} extend above a spatially homogeneous Freedericksz transition, where ***n*** bends away from the z axis. This bend produces symmetry breaking, since the ***n*** projection in the *xy* plane deviates along ± *y*. Such a symmetry breaking induces a texture transition, which can be considered as a super-critical pitchfork bifurcation between the Freedericksz transition and the EC instability, which is a typical feature for non-linear physical processes. We consider the ORs and cell-like EC patterns to be induced by the symmetry breaking and 'loss' of the electrical and optical anisotropies of the LC upon temperature variation.

For the R_{III} region, however, in addition to the symmetry breaking and the anisotropy 'loss' the smectic C fluctuations, existing below T^*, lead to a strong sign change of σ_a. The fluctuations affect a N's dynamic transport parameter, involving flow in the emerging layer structure. As a result, the bifurcation from the quiescent state to the EC state is sub-critical, with a large hysteresis (between the appearance and disappearance of the EC instability) and reflects a strong EC non-linearity.

The process of the closing of the rolls in localized dendritic states could be due to in-plane director rotation. The combination of such a complicated director ***n*** distortion in the presence of $U > U_{th}$, and the possibility that the electric charges move more easily in the layer planes, leads to a resultant charge distribution, which is inhomogeneous with respect to the ***n*** distortion in the *xz* plan. The corresponding torque, however, acts to increase the misalignment, thus leading the in-plane director to deviate significantly from the perpendicularity of the rolls. Such ***n*** behaviour could provoke spatio-temporal disorder of the EC pattern and dendrite motion, which we observed.

3. Conclusions

The Ns, which appears before S_C upon cooling, due to the strong smectic order fluctuations and surface symmetry changes imposed by the temperature variation, reveal ECs differentiated into three domains: (i) around the $T_{NI} - R_I$ with characteristics of the recently found isotropic prewave instability. This is due to both the 'loss' of σ_a anisotropy and a surface transition from a planar to a homeotropic orientation in the high-temperature N region; (ii) in the middle of the N temperature range, but above the temperature T^*, where the 'loss' of σ_a (still positive) is small, the R_{II} region is revealed. In this region, the smectic order fluctuations are not enough to change the classical-like character of the N. The EC pattern in the region R_{II} we called closed cell-like domains. The EC in this region partially follows the CH mechanism and the corresponding super-criticality in the competition between the Freedericksz and EC transitions; (iii) in the R_{III} region, where the sign of σ_a changes from positive to negative, the applied (normal to the substrate's planes) electric field induces a homeotropic orientation in the middle of the cell, while at the surface the initial planar orientation is retained. Such competition between the orientations in the bulk and at the surface, accompanied by σ_a 'loss', is the basis of the sub-critical bifurcation (between the appearance and disappearance of the EC instability) and the dendrite pattern formation in the R_{III} region.

Acknowledgements

This study was supported by Grant No.F-1307 from the Ministry of Education and Science of Bulgaria.

References

[1] P. G. de Gennes, J. Prost, The Physics of Liquid Crystals, 2nd ed., Oxford University Press, New York (1993).

[2] E. Dubois Violette, P. G. de Gennes, O. Parodi, J. Phys. (Paris) **32**, 305 (1971).
[3] L. Kramer, W. Pesch, in Pattern Formation in Liquid Crystals ed. A. Buka, L. Kramer, Springer-Verlag, New York (1996)
[4] H. Richter, A. Buka, I Rehberg, Mol. Cryst. Liq. Cryst. **251**, 181 (1994).
[5] J-H. Huh, Y. Hidaka, S. Kai, Phys. Rev. E **58**, 7355 (1998).
[6] S. Komineas, H. Zhao, L. Kramer, Phys. Rev. E **67**, 031701 (2003).
[7] J-H. Huh, Y. Hidaka, A. G. Rossberg, S. Kai, Phys. Rev. E **61**, 2769 (2000).
[8] J-H. Huh, Y. Yusuf, Y. Hidaka, S. Kai, Phys. Rev. E **66**, 031705 (2002).
[9] M. I. Barnik, L. M. Blinov, M. F. Grebenkin, A. N. Trufanov, Mol. Cryst. Liq. Cryst. **37**, 47 (1976).
[10] S. Kai, K. Hirakawa, Solid State Commun. **18**, 1573 (1976).
[11] P. Simova, M. Petrov, J. Phys. D **14**, 1 (1981).
[12] B. Katranchev, H. Naradikian, E. Keskinova, M. Petrov, J. P. Marcerou, Liq. Cryst. **31**(12), 1663 (2004).
[13] J. T. Gleeson, Nature **385**, 511 (1997).
[14] J. T. Gleeson, Phys. Rev. E **54**, 6424 (1996).
[15] N. Cheorghi, J. T. Gleeson, Phys. Rev. E **66**, 051710 (2002).
[16] L. Blinov, Electro-optical and Magneto-optical Properties of Liquid Crystals, The Universities Press, Belfast Ltd, Northern Ireland (1983).

*Corresponding author: mpetrov@issp.bas.bg